Vertical 3D nanostructures boost efficient hydrogen production coupled with glycerol oxidation under alkaline conditions

Shanlin Li[1, 2], Danmin Liu[1, *], Guowei Wang[1], Peijie Ma[1], Xunlu Wang[2], Jiacheng Wang[2, 4, 5, *], and Ruguang Ma[3,*]

[1] Key Laboratory of Advanced Functional Materials, Ministry of Education, Faculty of Materials and Manufacturing, Beijing University of Technology, Beijing 100124, China.

[2] The State Key Laboratory of High Performance Ceramics and Superfine Microstructure, Shanghai Institute of Ceramics, Chinese Academy of Sciences, Shanghai 200050, China.

[3] School of Materials Science and Engineering, Suzhou University of Science and Technology, 99 Xuefu Road, Suzhou 215011, China.

[4] School of Materials Science and Engineering, Taizhou University, Taizhou 318000, China.

[5] Hebei Provincial Key Laboratory of Inorganic Nonmetallic Materials, College of Materials Science and Engineering, North China University of Science and Technology, Tanshang 063210, China.

*Corresponding author. E-mail: dmliu@bjut.edu.cn; jiacheng.wang@mail.sic.ac.cn; ruguangma@usts.edu.cn

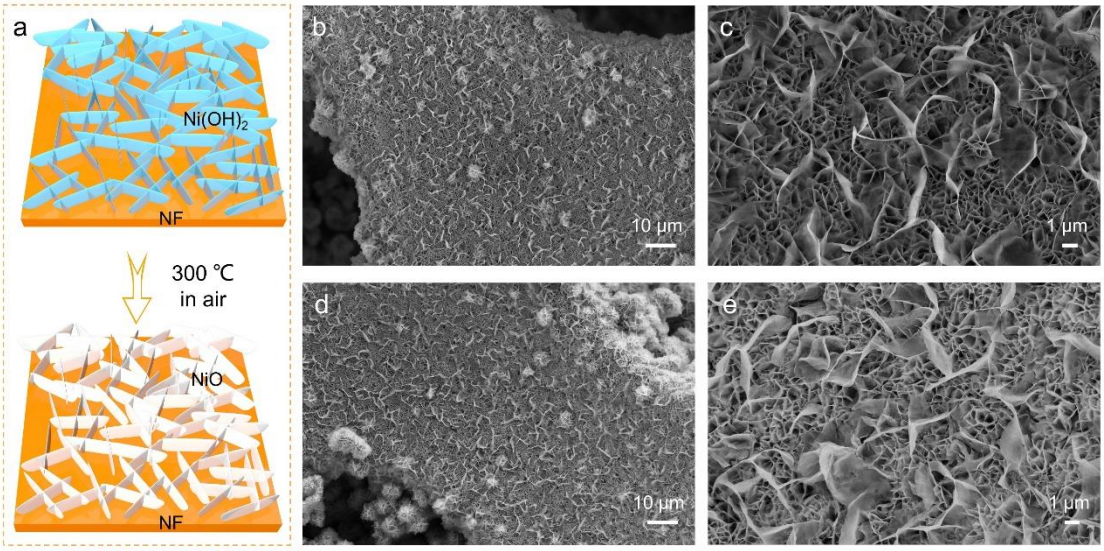

Fig. S1 (a) Schematic diagram of the synthesis of NiO. (b-c) SEM of $Ni(OH)_2$ on nickel foam (NF). (d-e) SEM of NiO on NF.

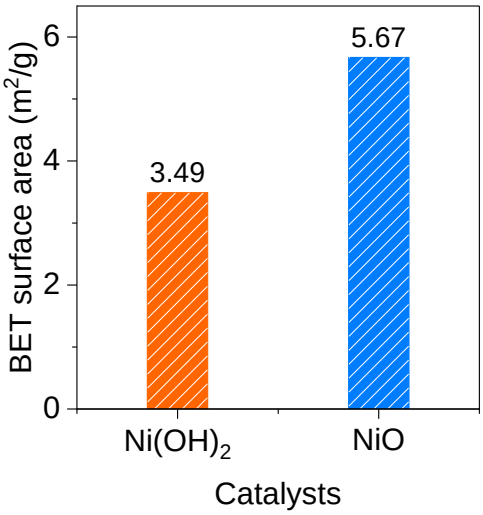

Fig. S2 BET surface area of the $Ni(OH)_2$ and NiO catalysts.

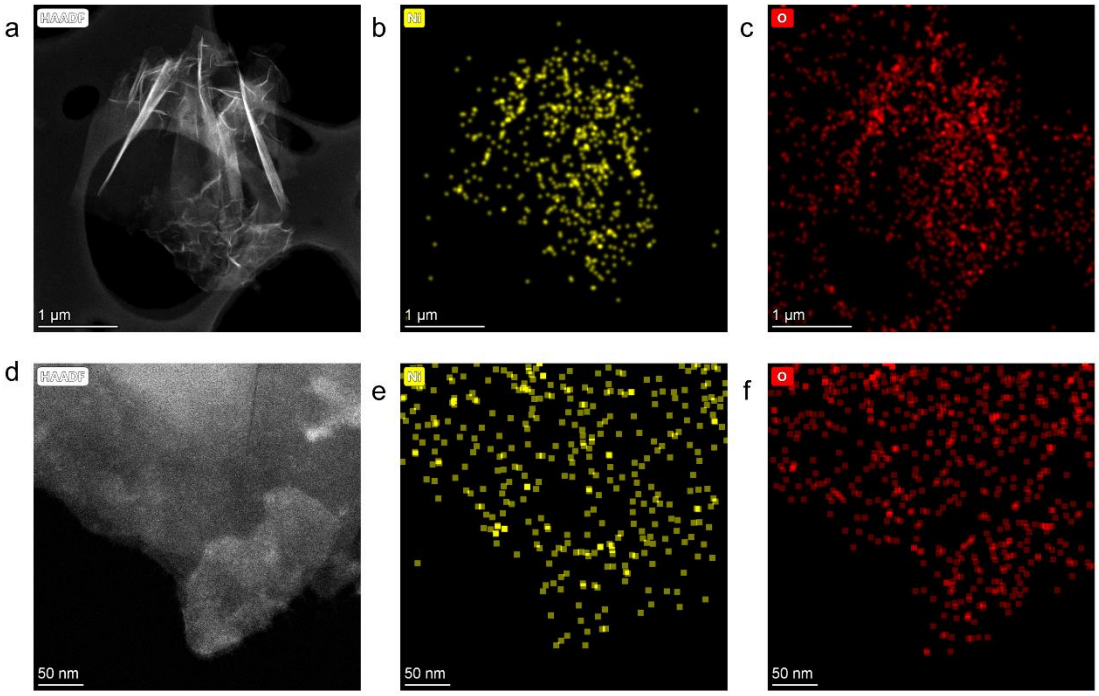

Fig. S3 HADDF-STEM images of $Ni(OH)_2$.

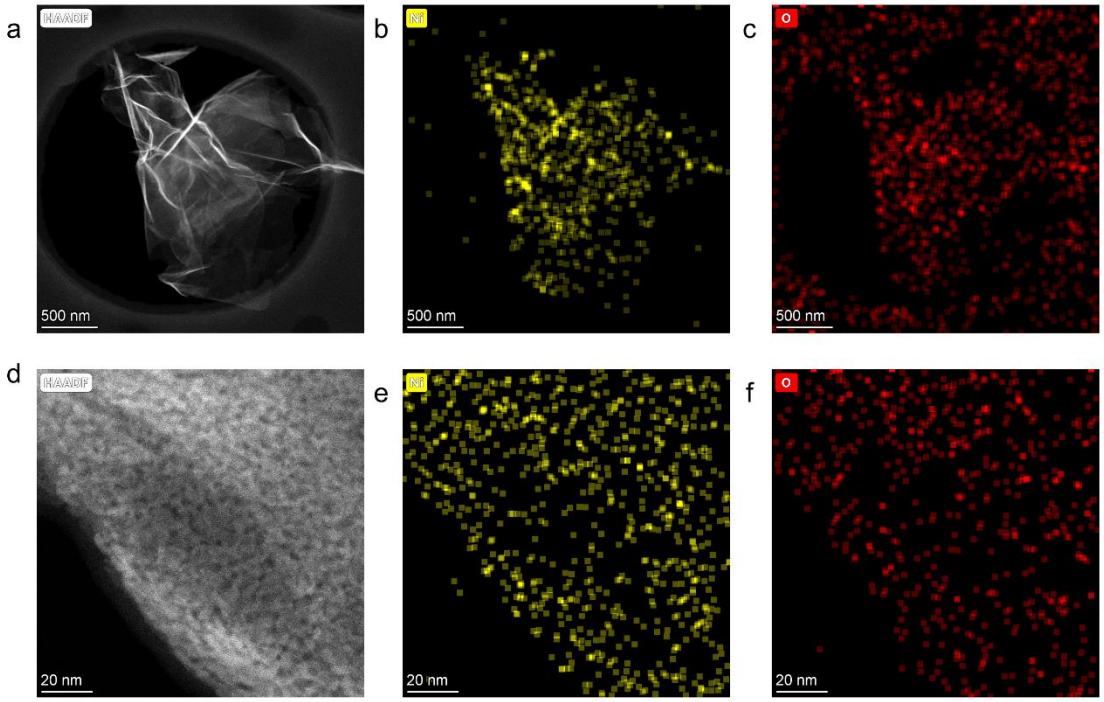

Fig. S4 HADDF-STEM images of NiO.

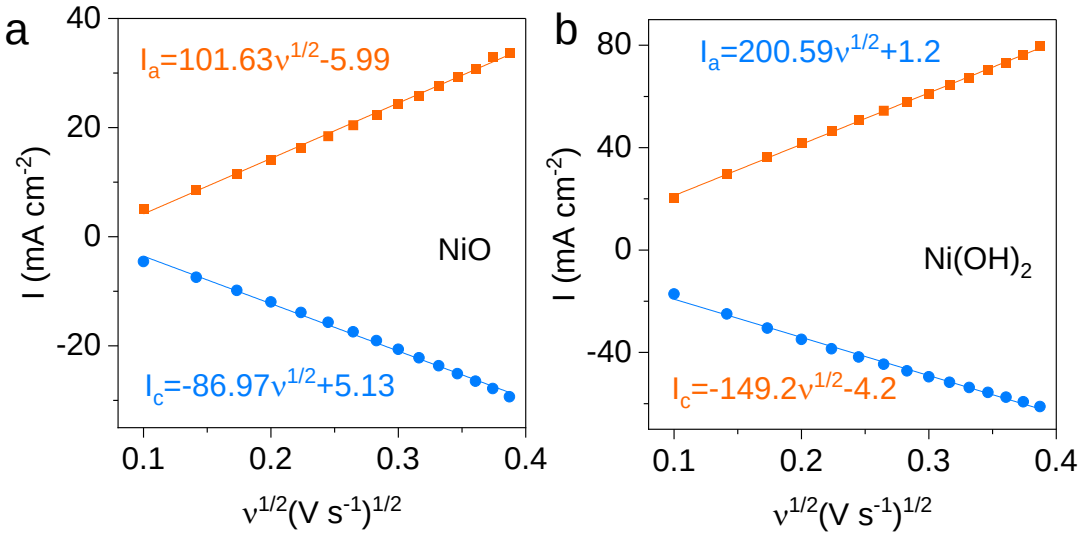

Fig. S5 Linear fitting of the anodic and cathodic peak current densities to the square roots of the scan rates for NiO (a) and $Ni(OH)_2$ (b).

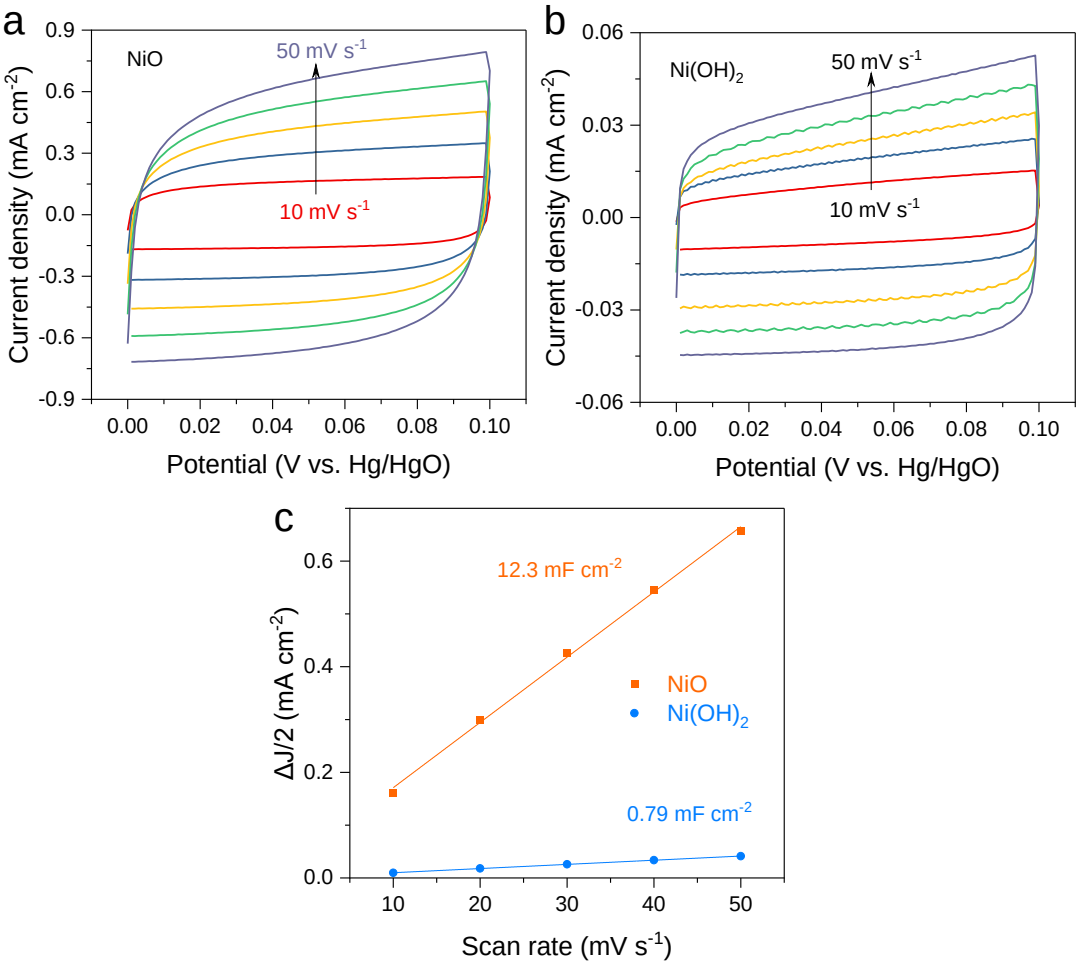

Fig. S6 ECSA data for NiO and $Ni(OH)_2$ in 1M KOH with 0.1 M glycerol. Cyclic voltammogram curves of (a) NiO and (b) $Ni(OH)_2$. (c) C_{dl} of corresponding electrocatalysts.

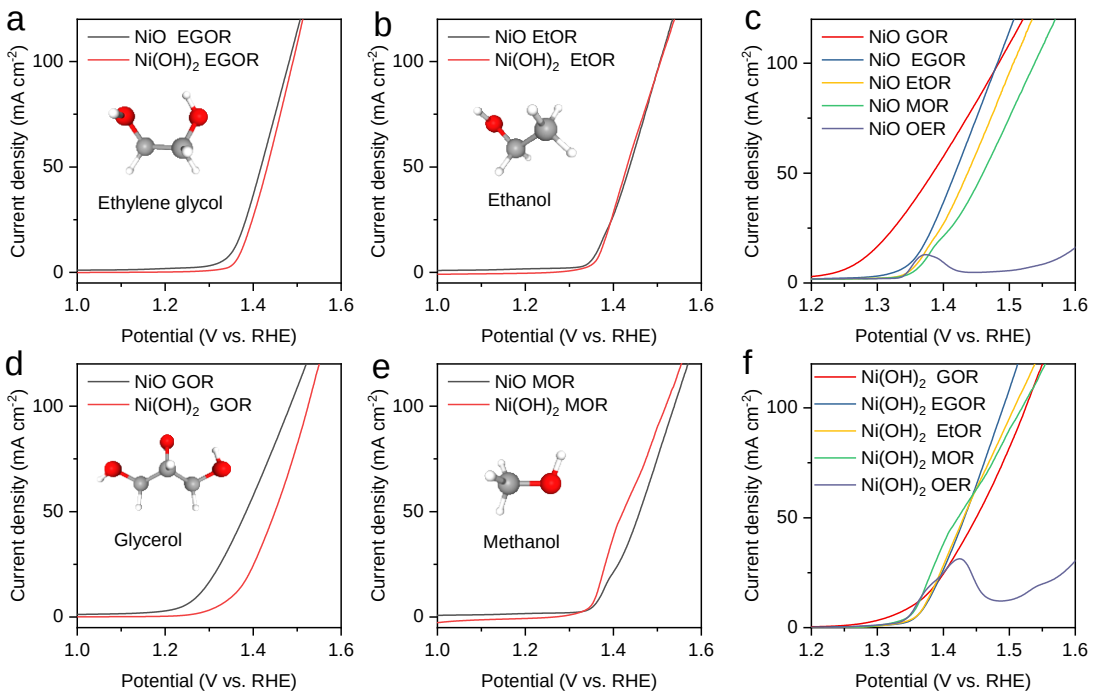

Fig. S7 The electrooxidation performance of other alcohols. LSV cures for ethylene glycol oxidation reaction (a), ethanol oxidation reaction (b), glycerol oxidation reaction(d), methanol oxidation reaction (e). LSV cures of alcohols oxidation reaction for NiO (c) and $Ni(OH)_2$ (d).

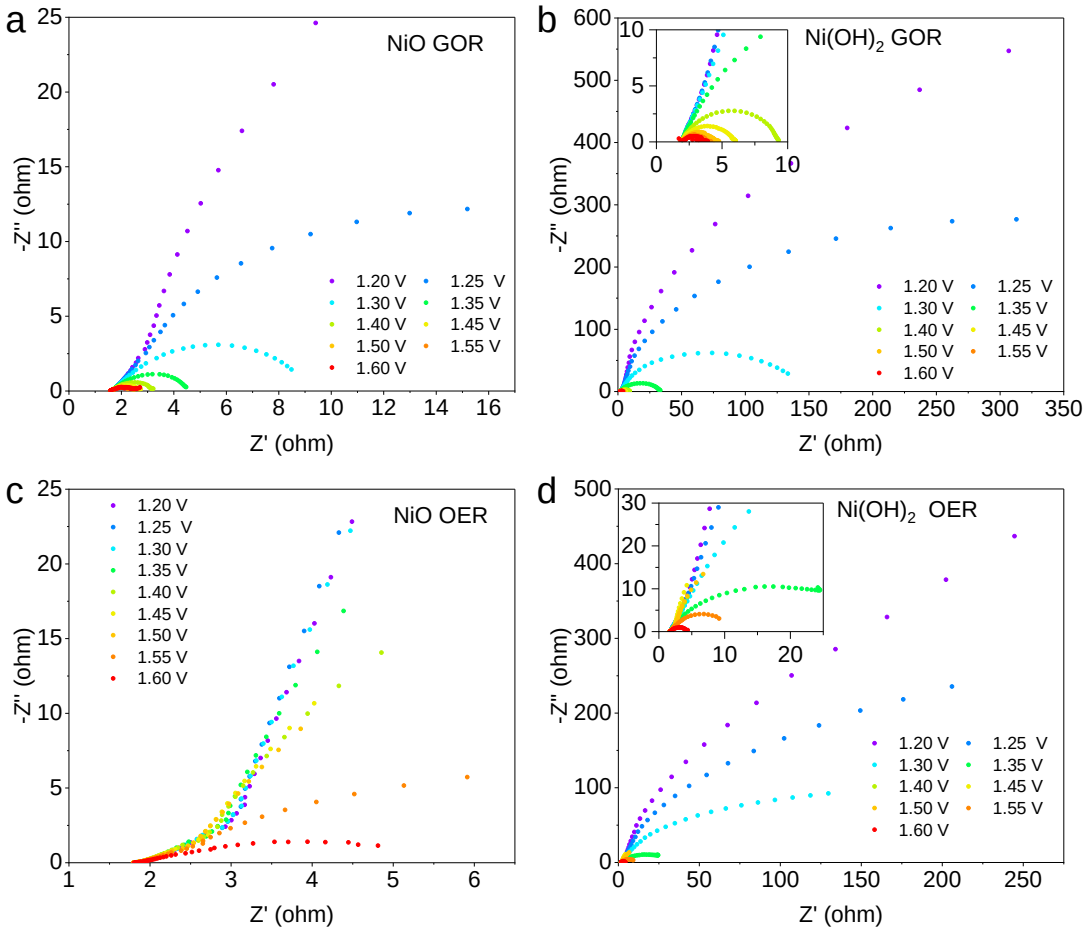

Fig. S8 In-situ EIS plots (Nyquist) of NiO and $Ni(OH)_2$ at different reaction conditions. (a) EIS plots of NiO under GOR. (b) EIS plots of $Ni(OH)_2$ under GOR. (c) EIS plots of NiO under OER. (d) EIS plots of $Ni(OH)_2$ under OER.

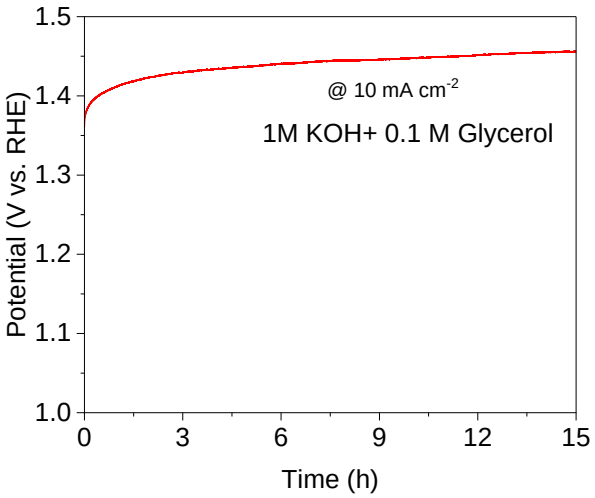

Fig. S9 Chronopotentiometric measurement of NiO in 1M KOH with 0.1 M glycerol.

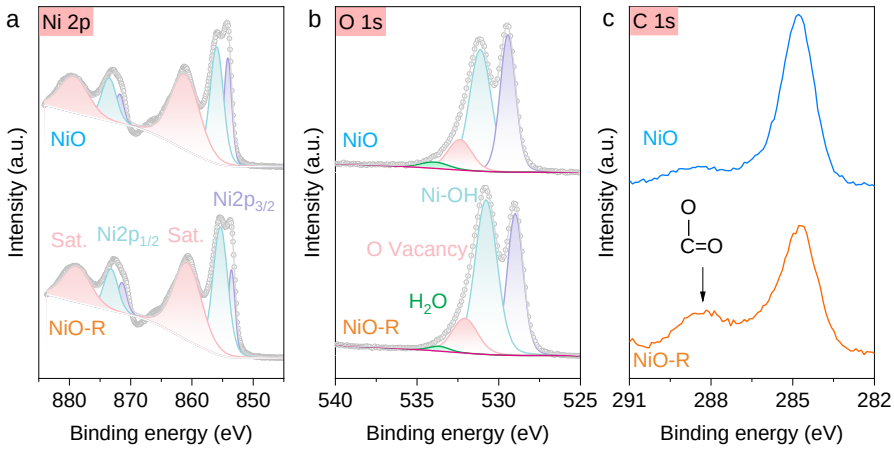

Fig. S10 High-resolution spectrum of Ni 2p (a), O 1s (b) and C 1s (c) of NiO before and after GOR, respectively.

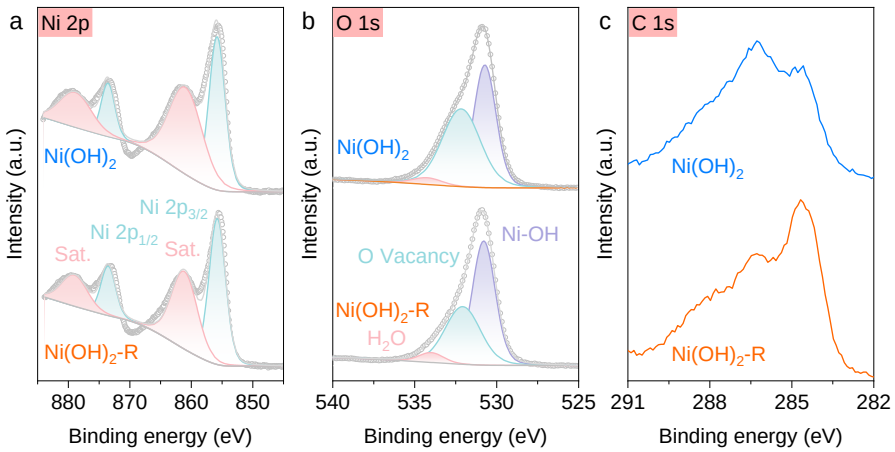

Fig. S11 High-resolution spectrum of Ni 2p (a), O 1s (b) and C 1s (c) of $Ni(OH)_2$ before and after GOR, respectively.

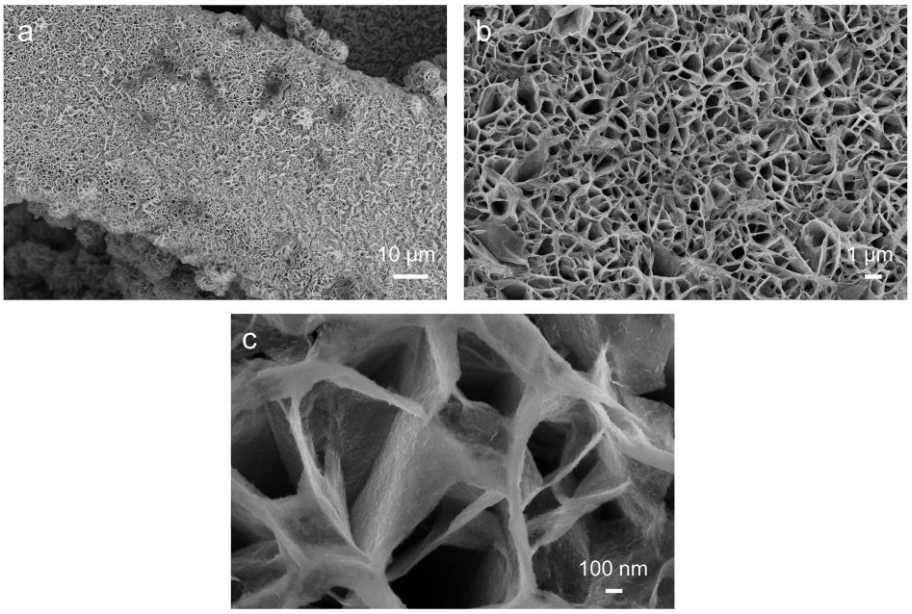

Fig. S12 SEM images of NiO after GOR.

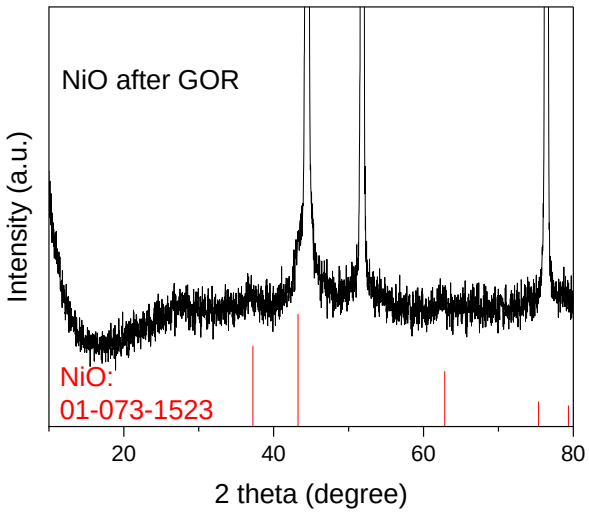

Fig. S13 XRD pattern of NiO after GOR.

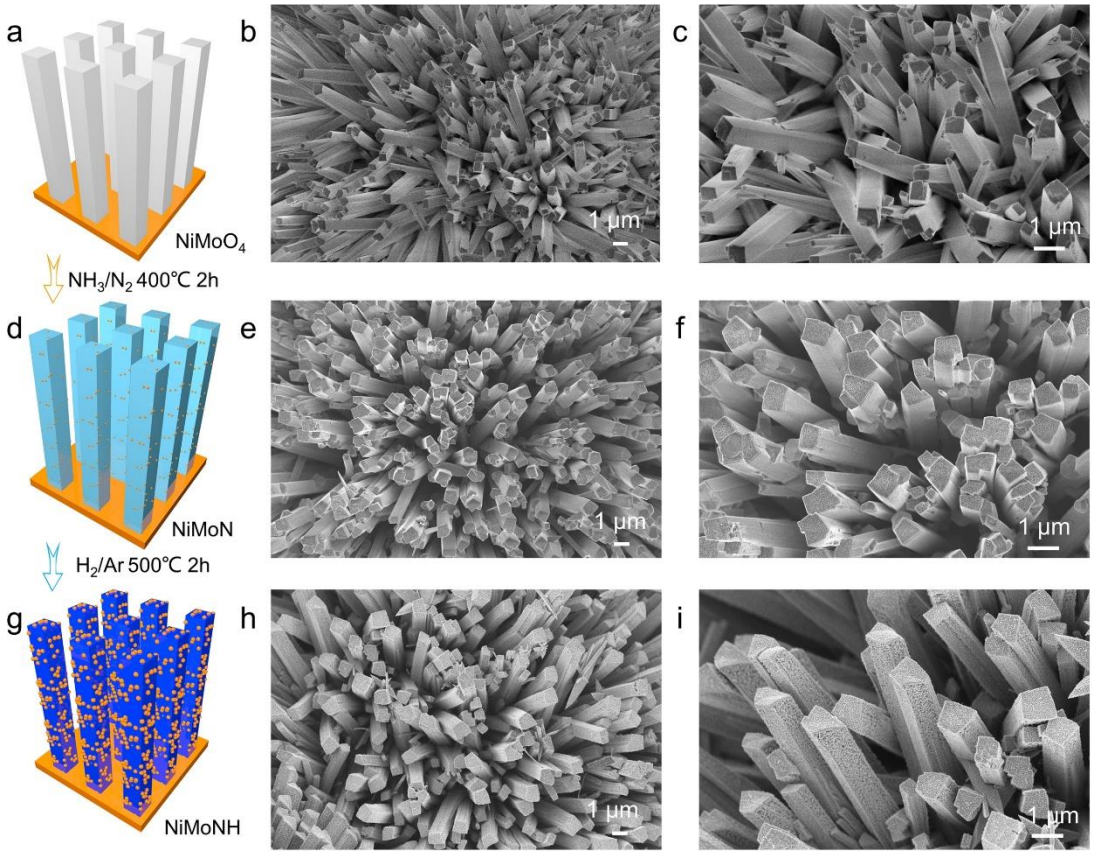

Fig. S14 Schematic illustration and SEM images of NiMoO (a-c), NiMoN (d-f) and NiMoNH (g-i).

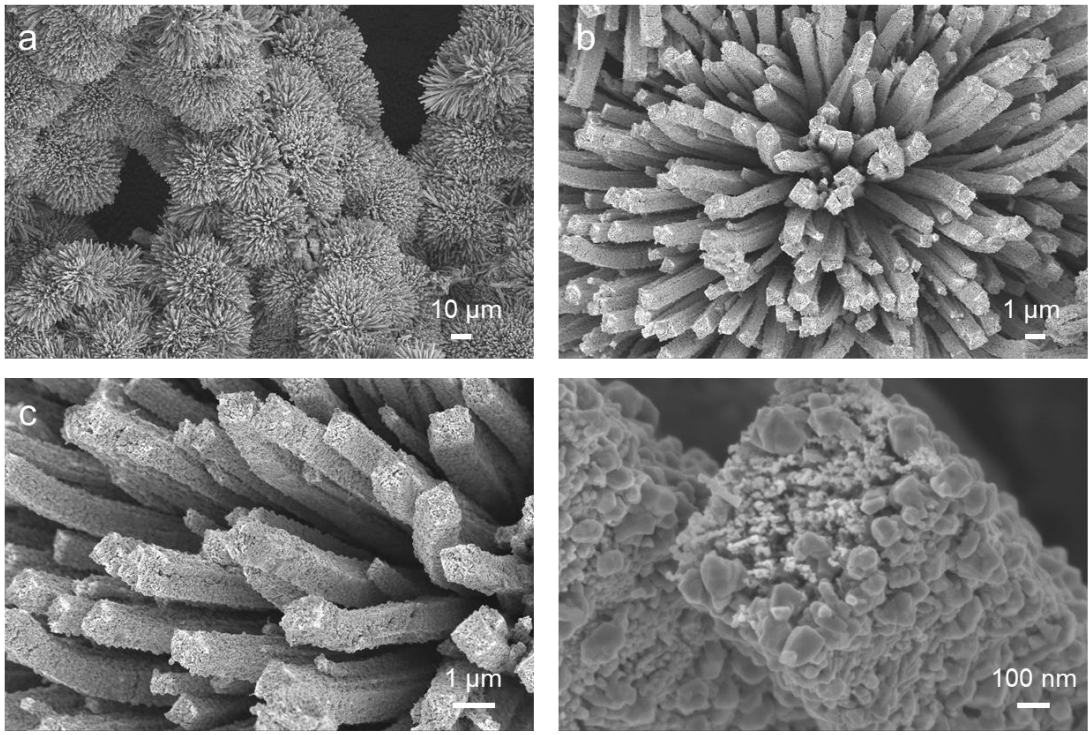

Fig. S15 SEM images of NiMoH (a-d).

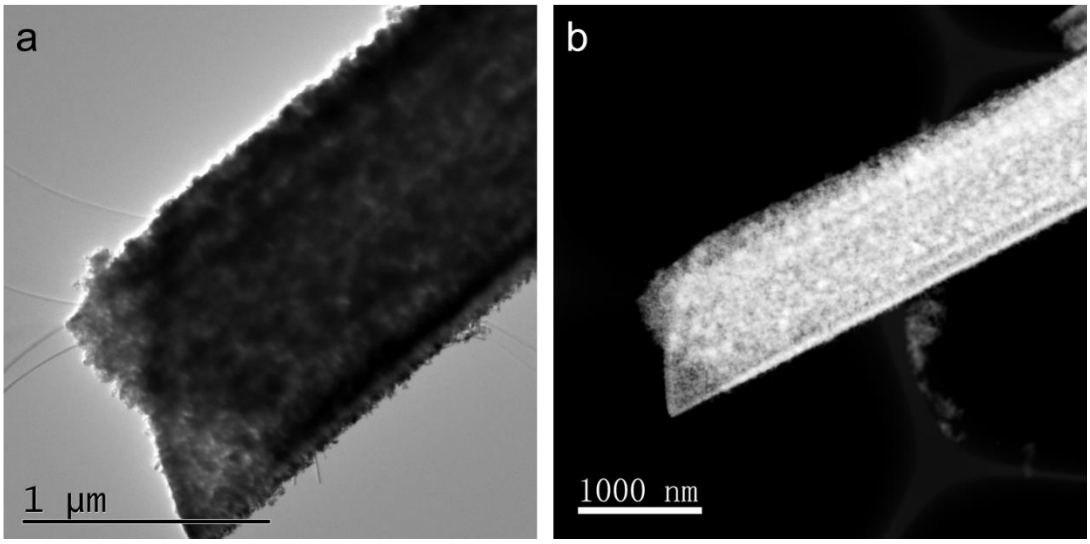

Fig. S16 TEM (a) and HADDF-STEM (b) image of NiMoNH.

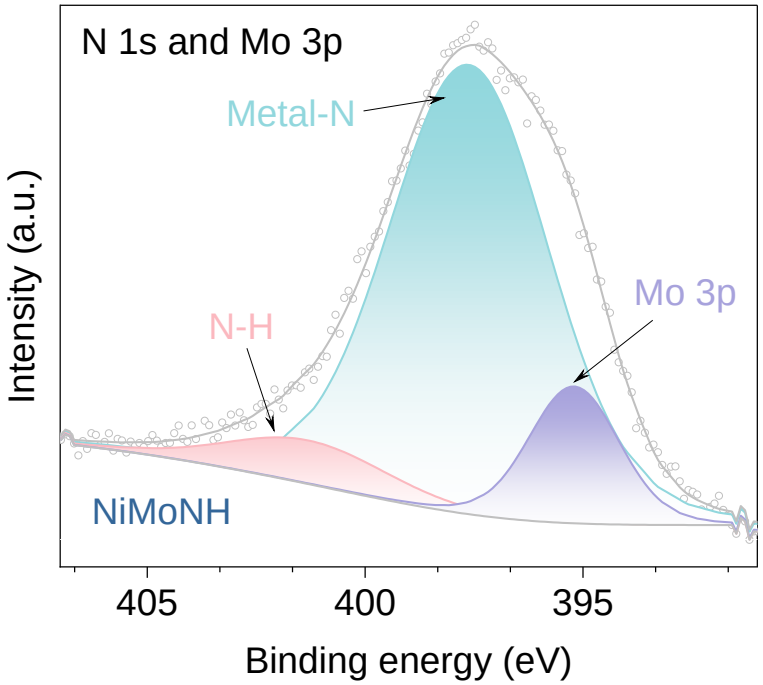

Fig. S17 High-resolution N1s and Mo 3p XPS spectra of NiMoNH.

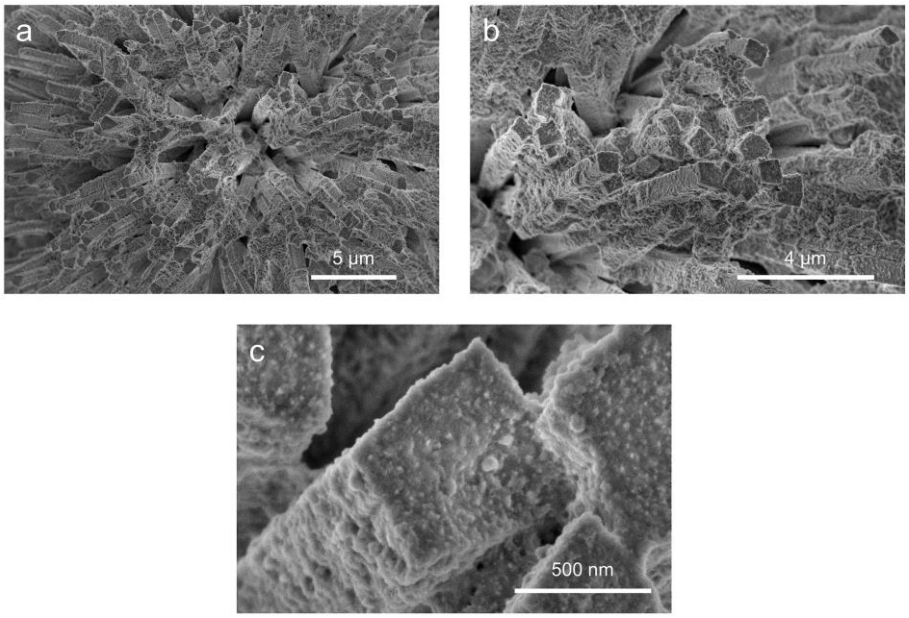

Fig. S18 SEM images of NiMoNH after HER.

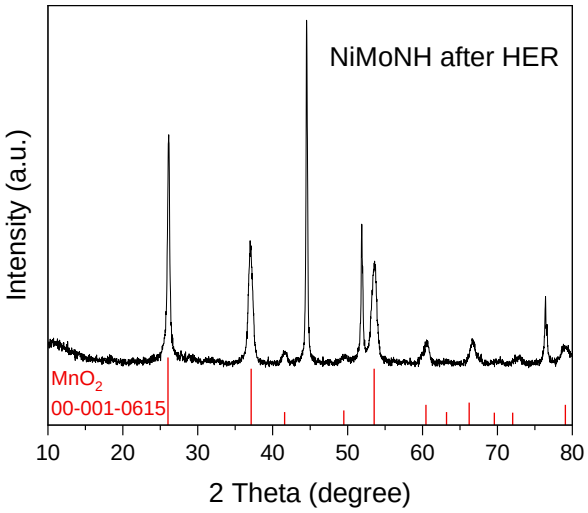

Fig. S19 XRD pattern of NiMoNH after HER.

Table S1. The GOR activity of transition metal-based electrocatalysts.

Electrocatalyst	Electrolyte	E_{GOR} [a]	E_{OER} [b]	ΔE [c]	Reference
NiO	1.0 M KOH with and without 0.1 M glycerol	1.3	1.59	293	This work
R-NiCuO	1.0 M KOH with and without 0.1 M glycerol	1.2	1.53	330	Energy Environ. Sci. 2022, 15, 3004.
CuCo-oxide	0.1 M glycerol in 0.1 M KOH	1.25	-	-	Adv. Mater. 2023, 35, e2203285.
CoNiCuMnMo-NPs/CC	1.0 M KOH with and without 0.1 M glycerol	1.25	1.55	300	J. Am. Chem. Soc. 2022, 144, 7224.
NiO_x/MWCNTs-Ox	1.0 M KOH with and without 1 M glycerol	1.31	1.59	280	ACS Catal., 2022, 12, 982-992.
Ni–Mo–N/CFC	1.0 M KOH with and without 0.1M glycerol	1.39	1.67	280	*Nat. Commun.*, 2019, 10, 5335.
CoNi film	1.0 M KOH with and without 0.33 M glycerol	1.3	1.6	300	*J. Hydrogen Energy 2022, 47, 32145.*

[a] E_{GOR} vs RHE at 10 mA cm^{-2} during the GOR; [b] E_{OER} vs RHE at 10 mA cm^{-2} during the OER; [c] E_{OER}-E_{GOR}.

Table S2. The HER activity of NiMo-based Electrocatalysts.

Electrocatalysts	Substrate	Electrolyte	Overpotential (mV) at 10 mA cm^{-2}	Tafel slope (mV dec^{-1})	Reference
MoO_2-Ni	NF	1 M KOH	47	36.6	ACS Catal. 2019, 9, 2275.
$MoNi_4$/MoO_{3-x}	NF	1 M KOH	17	36	Adv. Mater. 2017, 29, 1703311.
PS-MoNi@NF	NF	1 M KOH	30	37	Adv. Energy Mater. 2021, 11, 2003511.
N-$NiMoO_4$/NiS_2	carbon fiber cloth	1 M KOH	99	74.2	Adv. Funct. Mater. 2019, 29, 1805298.
Ni_2P/MoO_2/NF	NF	1 M KOH	34	45.8	Appl. Catal., B 2020, 269, 118803.
N-NiMoS	NF	1 M KOH	68	86	Appl. Catal., B 2020, 276, 119137.
$Ni_{0.2}Mo_{0.8}N$/Ni	NF	1 M KOH	14	33	Energy Environ. Sci. 2020, 13, 3007.
$MoNi_4$	NF	1 M KOH	15	30	Nat. Commun. 2017, 8, 15437.
NiMoNH	NF	1 M KOH+0.1 M glycerol	183 (100 mA cm^{-2})	146	This work.

Table S3. Comparison of performance of small molecule oxidation-assisted hydrogen production.

Catalyst	Electrolyte	Value-added product	potential at 100 mA cm^{-2}	Reference
hp-Ni||hp-Ni	10 mM Benzyl alcohol + 1M KOH	benzoic acid	1.66	ACS Catal. 2017, 7, 4564.
NiVRu-LDHs NAs/NF ||NiVRu-LDHs NAs/NF	1 M KOH + 0.1 M glycerol	Formate	1.62	Adv. Mater. 2023, e2300935.
Mo-Ni||Mo-Ni	10 mM Benzyl alcohol + 1M KOH	benzoic acid	1.53	J. Mater. Chem. A 2019, 7, 16501.
Co_3FeP_x||Co_3FeP_x	1 M KOH + 0.1 M glucose	-	1.59	Appl. Catal., B 2020, 263, 118109.
MoO_2-FeP@C||MoO_2-FeP@C	10 mM 5-hydroxymethylfurfural + 1M KOH	2,5-furandicarboxylic acid	1.69	Adv. Mater. 2020, 32, e2000455.
NiCo hydroxide || NiCo hydroxide	1 M KOH + 0.1 M glycerol	formate	1.58	Nat Commun 2022, 13, 3777.
NiMoNH||NiO	1 M KOH + 0.1 M glycerol	Formate	1.54	This work.